Innovative sol-gel coatings for corrosion protection of connector housings

Julien Acquadro, Sophie Noël, Pascal Chrétien, Frédéric Houzé, Philippe Teste, Clément Genet, Hiba Hazougaghe, Florence Ansart, Marie Gressier, Marie-Joëlle Menu, et al.

Innovative sol-gel coatings for corrosion protection of connector housings

J. Acquadro[1], S. Noël[1], P. Chrétien[1], F. Houzé[1], Ph. Testé[1], C. Genet[3], H. Azougaghe[2], F. Ansart[2], M. Gressier[2], M.J. Menu[2], R. Montpellaz[3], O. Gavard[3], R. Leroy[4], G. Trédan[4], S. Demarthon[5], T. Pichot[5], F. Raoul[6], M. Ladiré[6]

[1] Université Paris-Saclay, CentraleSupélec, CNRS, Laboratoire de Génie Electrique et Electronique de Paris, 91192, Gif-sur-Yvette, France,
Sorbonne Université, CNRS, Laboratoire de Génie Electrique et Electronique de Paris, 75252, Paris, France
[2] Université Toulouse 3 – Paul Sabatier, Laboratoire CIRIMAT, UMR CNRS 5085, Toulouse, France
[3] Amphenol Socapex, 948 Promenade de l'Arve, BP29, 74311 Thyez Cedex, France,
[4] Radiall, 642 rue E. Romanet 38340 Voreppe, France,
[5] Souriau ITD EATON, 89, route de Saint Hubert, 72470 Champagné, France,
[6] TE Connectivity, 17 rue Lavoisier, 27000 Evreux, France.

***Abstract*— This paper presents the electrical properties of innovative sol-gel coatings for connectors. A first study has shown the feasibility of developing a conducting and anti-corrosion coating for connector housing based on sol-gel chemistry. Such coatings aimed at replacing cadmium and chromium (VI) as recommended by REACH and RoHS regulations must have equivalent properties. A large consortium has been established in order to tackle aspects of the project from the formulation, the characterizations and the scale-up phases. The electrical properties of the coatings are obtained with conductive fillers of various types. We present here electrical characterizations both at the macroscopic scale and at the microscopic scale and try to correlate the conduction to the various parameters involved in the complex mechanisms ruling the film formation.**

Keywords; aluminum, corrosion protection, cadmium, chromium VI, sol-gel coating, carbon fillers, electrical conduction.

I. INTRODUCTION

Trioxide of chromium (Cr(VI)) passivated cadmium has been used for years to provide efficient anti-corrosion protection of aluminium housings of harsh environment connectors; it also possesses good conduction, low friction and self-healing properties.

Many harsh environment aerospace connectors, for example the circular 38999 type, have an aluminium housing coated by high phosphorous nickel (NiP) with a final coating of chromium VI passivated cadmium (Cr(VI) passivated Cd).

Cr(VI) has been a substance of very high concern (SVHC) since 2010 for the European Union; it was then registered by ECHA in annex 14 in 2011 [1]. Since 2017 its use has been banned by REACH regulations unless an exemption was applied for, obtained and substitution plans proposed [2].

In this context, many studies have taken place to find REACH and RoHS compliant ways of protecting aluminium surfaces. An extensive literature review was published by Mitton [3]. Among the various substitutions proposed an interesting one is the use of the sol-gel process for the fabrication of an anti-corrosion coating [4].

The sol-gel process has been known for several years; it involves the transition of a system from a liquid “sol” phase into a solid “gel” phase. The sol-gel process can be summarized as hydrolysis and polycondensation of precursors [5].

Specifications for such a coating include dark color, low friction, anticorrosion and electrical conduction properties.

Conducting sol-gel coatings can be obtained by adding conducting fillers in the sol but requires much attention.

The choice of precursors and type of conducting filler as well as the formulation and process parameters are critical to obtain a coating with specific properties.

It was shown by Genet et al. in [6-8] that by adding carbon-based fillers to a well-chosen formulation a coating with anticorrosion and conduction properties could be obtained. This work showed the feasibility of the process

GPTMS [(3-Glycidyloxypropyl)trimethoxysilane)] and TPOZ [zirconium (IV) propoxide] were chosen for precursors, see Fig.1.

A sol was obtained by mixing the GPTMS and TPOZ precursors to water, additives and carbon fillers.

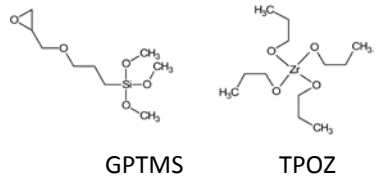

Fig.1: The precursors selected for the sol.

The additives were acetic acid and surfactants. After an homogenization and stirring step the sol was stored for a maturation period during which the chemical reactions lead to the gel formation. The process is described in Fig.2.

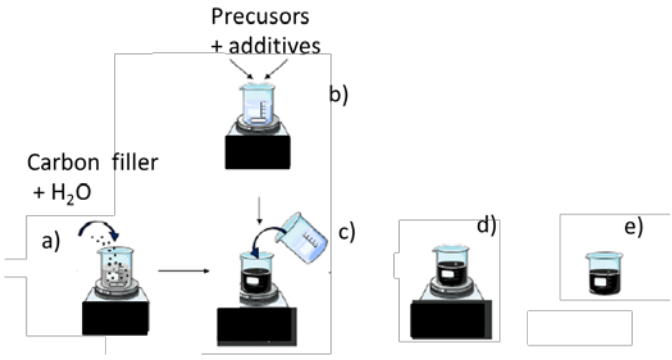

Fig.2: Sol preparation a), b, c). Dispersing d) and maturation e). The coupons are then dip coated in the matured sol.

The deposition technique chosen was the dip-coating because of its easy implementation and the possibility to obtain controllable coatings [9]. The samples were dip coated in the matured sol and then submitted to a double heat treatment first to eliminate the remaining solvents and then for the final consolidation of the coating.

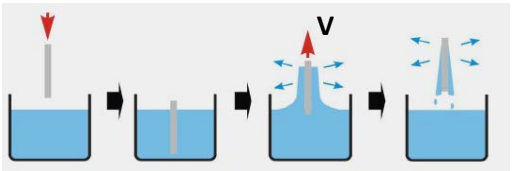

Fig.3: Dip coating of the substrates. The coupon is withdrawn at constant speed V.

In their study the authors succeeded in depositing carbon charged sol-gel coatings on high phosphorus nickel coated Al 6061-T6 samples by the dip coating method. The coated coupons where characterized by various means: good adhesion to the substrate was found as well as enough conductivity and corrosion protection during neutral salt spray (NSS) tests (ISO 9227-2017). This accelerated corrosion test allows evaluating the suitability of a coating for use as a protective finish. The neutral NSS conditions were: salt solution 5%w NaCl, flow 1 to 2 $mL.h^{-1}$, T 35°C, pressure 0.9 bar. Coupons showed no degradation after 500h. Electrical continuity was obtained before and after the test.

Fig.4: Connector housing coated with the charged sol-gel process [8]

The dipping process was then applied to connector housings. Fig. 4 shows the aspect of such a deposition.

Following this proof of concept, several connector manufacturers have launched a project called CadSTAR to investigate the adaptation of the sol-gel process to the possibility of an implementation to industrial lines.

To work on this aspect several parameters of the first formulation had to be changed to comply with REACH, RoHS and safety measures. For example, surfactant additives had to be changed to comply with RoHS directives. This paper describes the efforts made to improve the formulation in view of industrial requirements.

II. EXPERIMENTAL

A. Samples

1) *Substrates*

The samples were aluminum 6061-T6 coupons (80mmx40mmx1mm) coated by 20µm of high phosphorus nickel; the surfaces were cleaned and activated by an acidic bath and thoroughly rinsed before the deposition process.

2) *Carbon fillers and sol*

The first results had been obtained with a carbon black (CB) filler to achieve conductivity of the sol-gel coating. This filler was a powder (Imerys) and had to be replaced by water-based carbon suspensions which were purchased from Imerys. The consequence was that the compositions of the suspensions, being commercial, were not totally known. In the sol preparation (Fig.2), instead of mixing water and CB powder, water was added to the suspension. As a result the viscosities of the sol were very low (between 2 and 3 mPa.s). Two types of coatings are investigated here.

The precursors were the same as described above [7-8]. Important parameters for the sol-gel process are the ratio of hydrolysis, the proportion of GPTMS to TPOZ and the proportion of conducting filler. The ratio of hydrolysis, is defined as H= $n(H_2O)/(3nGPTMS+4nTPOZ)$; its value was not changed. The proportion of GPTMS to TPOZ (ratio of Si/Zr) was the same. The proportion of conducting material is

defined as the mass of conducting material M_{cond} to the mass of insulating material M_{ins}. M_{cond}/M_{ins}=1 was chosen as in the previous study.

The dip-coating of the coupons in the matured sol was performed at constant speed. After that a two-step thermal treatment was applied to the coated coupons.

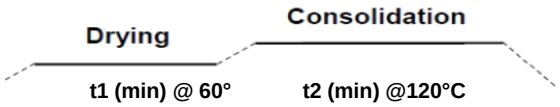

Fig.5: Two step heat treatment

Coatings were made from the above described sol-gel charged with two types of suspensions ([A] and [B]).The speed of withdrawal of the coupons during the dip-coating process was varied as well as the duration of the consolidation phase. The results for two coatings called [A] and [B] are presented here. They involved suspensions [A] and [B] which contain different types of carbon fillers.

B. Deposition process

A constant speed Bungard Electronik RDC 21-K dip coater was used. The slabs were dipped into the gel and then withdrawn at constant speeds of 100mm/min, 200mm/min, 300mm/min and 600mm/min.

C. Consolidation duration

After dip-coating the coated slabs were heat-treated, first at 60°C for 60min in order to eliminate the solvents and then at 120°C for the consolidation of the coating. Durations of the second step were varied from 30 to 240min.

D. Characterization techniques and experimental test

1) *Topography*

3D images were acquired with a Bruker Contour GT-X 3D Optical Profiler and surface roughness parameters were calculated with the device software.

TEM images were acquired with a JEOL JEM2100F.

2) *Electrical characterization*

a) 4 point resistivity measurements :

Electrical measurements were performed with a Signatone Pro4 4-point probe resistivity device; the four point probe head specifications are: 1.587 mm tip spacing, 0.254 mm tip radius and 45 gf normal load on each tungsten carbide tip. A Keithley 2400 sourcemeter and a 2182A nanovolmeter were used to measure the sheet resistance. The aim was to assess the macroscopic conductivity of the coatings; therefor specific samples were made on glass slabs in order to have an insulating substrate and measure the properties of the coating only.

b) Conductive probe AFM

AFM topography and electrical maps were obtained with a Bruker MultiMode8 equipment fitted with a special home-made amplification and conversion device, called Résiscope (referred to as CP-AFM) in order to acquire simultaneously topographic and electrical images of the surfaces using doped diamond coated tips (radius ≈ 150 nm). The intrinsic resistance of these probes is about 5 kΩ. The aim was to have a local evaluation of the conduction in relation to the topography.

3) *Corrosion behaviour*

Neutral salt spray (NSS) was performed with an Ascott S12IS model according to NF-EN-ISO-9227 and ASTM-B117 (solution of 5% NaCl in H_2O). The coupons are protected with 3M Teflon tape on one side and on the edges. Samples are checked daily for the presence of pits.

III. RESULTS AND DISCUSSION

All the coatings were deposited both on NiP coated aluminium coupons and on glass slabs.

A. Coating [A]

For coating [A] (suspension [A]) the carbon charge is a mixture of carbon black and graphite in a water suspension. Fig.6 is a TEM image of the particles; it shows the mixture of very small spherical particles of carbon black (as small as 50nm in diameter) between or on large thin sheets of graphite.

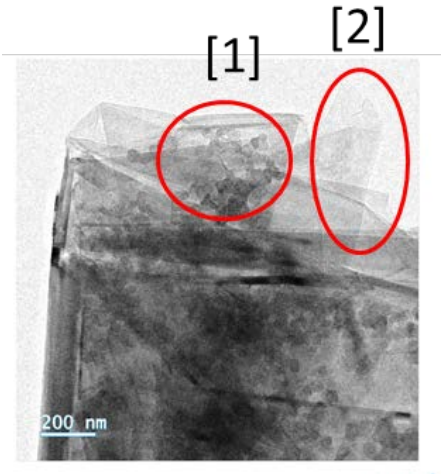

Fig.6: TEM image of the suspension [A] deposited on a grid (20kV) showing overlapping large graphite sheets with in zone [1] carbon black particles and zone [2] part of the graphite sheets alone.

The influence of the withdrawal speed *V* during the dip-coating process was investigated. This speed is known to influence the thickness of the coating. For a Newtonian fluid the thickness *e* of the coating is related to $V^{2/3}$ in the Landau Levitch equation [10].This equation involves also the viscosity of the fluid which is very low; as a consequence, the thickness of the coatings was measured to be around 300 to 500nm. Whether a suspension of sol-gel and carbon filler can be considered as Newtonian is difficult to answer and to be investigated.

The optical observation of the coated Al samples shows that the deposition process was rather uneven with probably excess sol-gel on some places and accumulations of graphite flakes on other ones. Some areas had a clear aspect while others had a dark one; an example is shown in Fig.7. This was confirmed by the observation of the surfaces by conducting tip AFM. We show here the results for a clear and a dark zone for coating [A] in the standard conditions of dip-coating and consolidation (300mm/min and 120min at 120°).

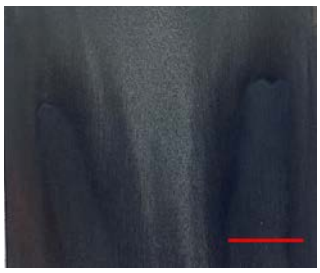

Fig.7: Example of clear and dark zones observed on sol-gel [A] coatings; red scale:10mm.

Fig.8 shows a view of the surface of the sol-gel coating [A] acquired with the conducting-tip AFM. It shows the presence of excess sol-gel matrix, in zone [1], graphite plates in zone [2] and carbon black rich matrix in zone [3]. The most conducting zones correspond to carbon black rich areas; the graphite plates show lower conductivity. Calculating the average log resistance over the whole image (512x512 measurements matrix) gives <LogR>=7.20 . Fig.8 corresponds to a clear zone.

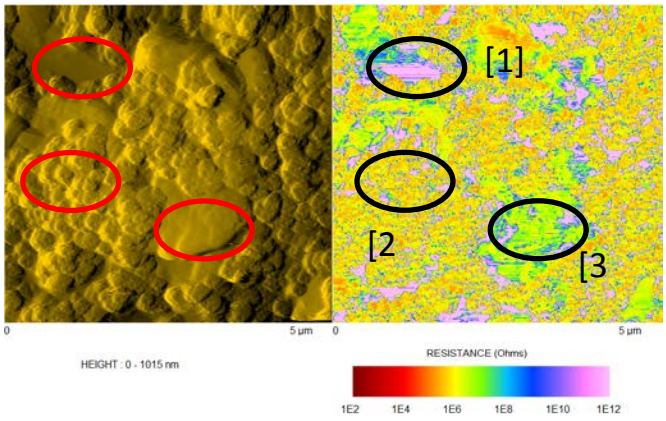

Fig.8: AFM images of sol-gel [A] coating on NiP/Al substrate (300mm/min, 120min-120°)- clear zone. Left) topographic image, right) electrical image; doped diamond tip, 150nN normal load. Tip-surface resistance scale. Calculated mean log resistance <LogR>=7.20

A dark zone is shown in Fig.9. These dark zones are less rich in carbon black therefore less conducting and <LogR>=8.66 for the shown image.

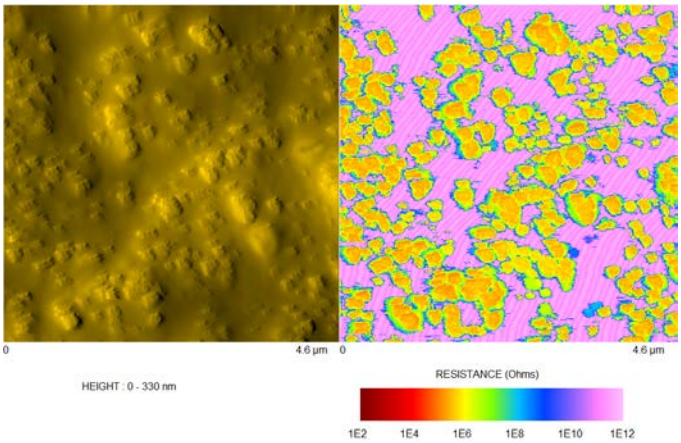

Fig.9: AFM images of sol-gel [A] coating on NiP/Al substrate (300mm/min, 120min-120°)- dark zone. Left) topographic image, right) electrical image, doped diamond tip, 150nN normal load. Tip-surface resistance scale. Calculated average log resistance <LogR>=8.66

The roughness of the various coatings was measured on many locations. The roughness parameters were calculated on the whole analyzed surface after appropriate filtering. *Sa* is the surface average roughness (arithmetic mean of the absolute heights) and *Sz* is the peak to valley height. In this paper images of 127µmx95µm were taken and the filter was λ_c=0.025µm. The values of *Sa* and *Sz* are shown Fig.10 and Fig.11.

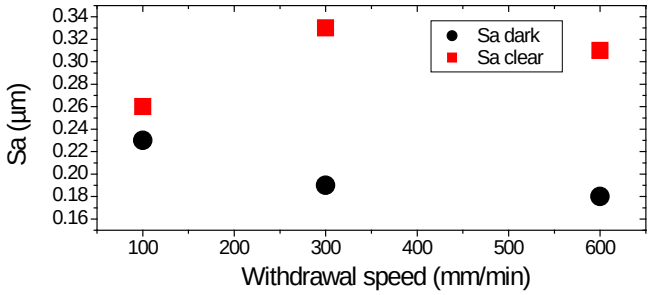

Fig.10: *Sa* roughness parameter for coating [A] deposited at different withdrawal speeds (NiP/Al substrate). The surface displays clear zones and dark zones.

Fig.10 shows that the dark zones have a lower average roughness and that the trend is the same for all the withdrawal speeds. The *Sz* values of Fig. 10 follow the same trend. Note that the sol-gel coating is deposited on NiP. Roughness measurement (on the non-activated surface) gave *Sa*=0.19µm and *Sz*=2.17µm. The observation that *Sa* values for 300 and 600mm/min for dark areas (Fig.10) are the same values as for the bare nickel can be explained by a thicker layer in which graphite plates are either less numerous or embedded so that the surface is smoother. This would not be observed for the 100mm/min coating since low speed means lower thickness. This is in agreement with the AFM topographic images that show more protruding graphite plates on the clear zones (Fig.8). Thanks to the electrical images it is easy to distinguish graphite from carbon black. The *Sz*

parameter involving the highest peak to valley values on the whole surface are more prone to defects.

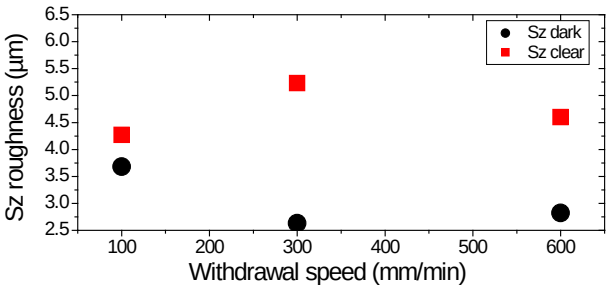

Fig.11: *Sz* roughness parameter for coating [A] deposited at different withdrawal speeds (NiP/Al) substrates. The surface displays clear zones and dark zones.

The electrical conduction of the coatings was assessed. The microscopic conduction could be visualized on the AFM images of Fig.8 and Fig.9 but a more macroscopic measurement is needed to measure the conductivity of the coatings. This was achieved by measuring the sheet resistance *Rs* of the coatings on an insulating substrate (glass) with the 4 point device.

Fig.12: Charged sol-gel coating deposited on glass at constant speed showing the locations of *Rs* measurements.

Three samples were analysed, each coated on both sides by dip-coating at different withdrawal speeds. Columns of 10 to 15 measurements were performed on each side (as illustrated in Fig.12).

Plotting the different values versus the position can thus give an indication on the evolution of the coating thickness and/or the distribution of charges in the coating.

Fig.13 shows the results of the 4 point sheet resistance measurements. Data were taken along in columns from top to bottom. Care was taken to discard very high values of resistance that could be erroneous. A line of measurement was taken into account when all the values were correct thus attesting of an even deposit. Fig.13 shows the average, the minimum and maximum values of *Rs* along these lines. For the smallest *V* value (100mm/min) the average value of *Rs* is 27 567Ω□; it is the highest of the series. The values of minimum and maximum *Rs* show that the distributions of fillers in the coating are not even. Increasing the value of *V* initially diminishes the surface resistance value. The minimum *Rs* (1910 Ω□) has the lowest value for *V*=300mm/min. For higher speed (600mm/min) the average *Rs* is higher (5741 Ω□) and the dispersion of the values is much higher; the minimum value is the lowest: *Rs*=1176Ω□. At this speed the film should be thicker according to the Landau Levitch equation but the deposition process of the suspension involving charges of various sizes is complex.

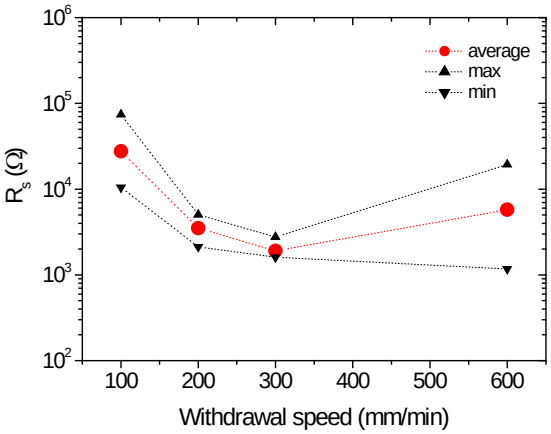

Fig.13: Maximum, minimum and average values of *Rs* for different withdrawal speeds for coating [A]. (Heat treatment 60min at 60°C and 120min at 120°C).

In order to evaluate the conductivity of the coating without the influence of the deposition mechanism, it is interesting to determine the minimum value of *Rs* for the entire set of measurements which is plotted Fig.14.

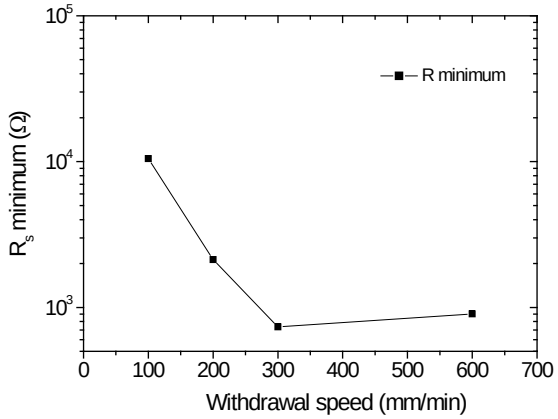

Fig.14: Minimum *Rs* value from all the data for various withdrawal speeds. Heat treatment 60min at 60°C and 120min at 120°C.

This value is purely linked to the local organization of the carbon charges and the sol-gel network. The minimum value is 735Ω□ for *V*=300mm/min. Supposing that the thickness of the coating is 500nm (the thicknesses of the

coatings have been measured to be between 300 and 500nm by scanning electron microscopy (SEM) observations of FIB milling cross-sections), the resistivity of the coating would be 3.6 10^{-4} Ω.m which is a rather low value.

At low deposition speed (100mm/min) the quantity of charged sol-gel dragged on the coupon is smaller and the carbon particles have rather similar movements. The dark and light zones have about the same *Sa* and *Sz*. For higher withdrawal speeds (300mm/min) some areas have more sol-gel and carbon black (dark ones) and some have more graphite (light ones). This is consistent with the higher and more scattered values of *Rs*. It seems that for this formulation the speed value of 300mm/min is a good compromise between two mechanisms occurring during the dip-coating.

The influence of the duration of the consolidation at 120° treatment was investigated for *V*=300mm/min. The value of 120° was determined from thermo-gravimetric differential thermal analyses (TG-DTA) performed on various sol and xerogel. [6]. The duration of the consolidation plateau was varied from 30min to 240min. The optical aspect of the samples both on Al and on glass was not modified.

The observations of the surfaces with the conducting AFM showed images with the three types of features: the matrix, the graphite plates, the carbon black rich area. The electrical images of the clear zone show there is no effect of the heat treatment duration while the electrical behaviour of the dark regions is affected. This can be seen by comparing the 60min (Fig.15) to the 240 min (Fig.16) treatments. The <LogR> value for 60min is 8.84 while it is 9.83 for the 240min one.

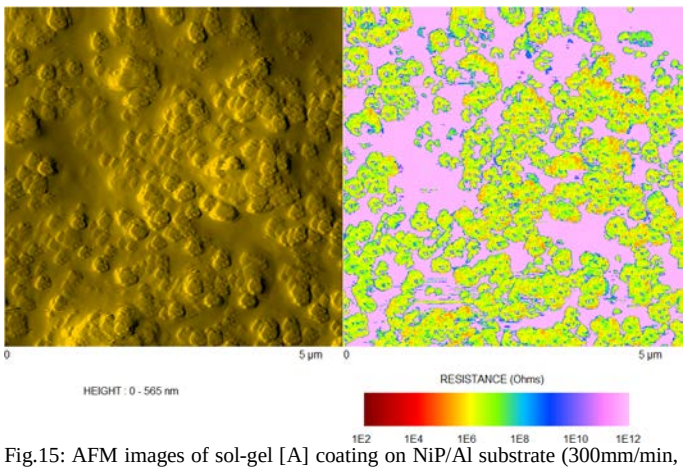

Fig.15: AFM images of sol-gel [A] coating on NiP/Al substrate (300mm/min, 60min-120°)- dark zone. Left) topographic image, right) electrical image, doped diamond tip, 150nN normal load. Tip-surface resistance scale. <LogR>=8.85.

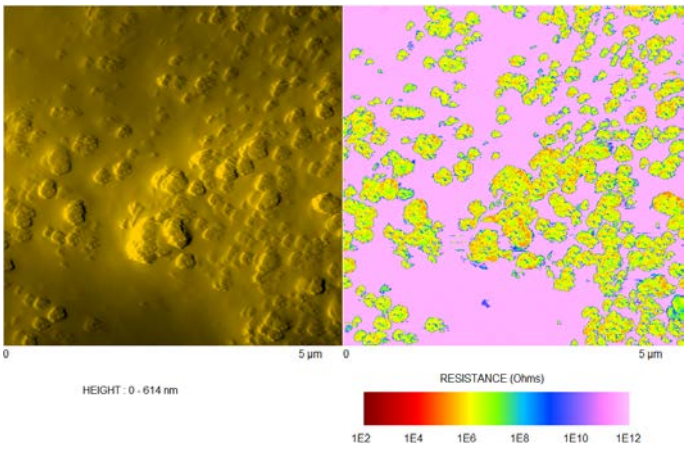

Fig.16: AFM images of sol-gel [A] coating on NiP/Al substrate (300mm/min, 240min-120°)- dark zone. Left) topographic image, right) electrical image, doped diamond tip, 150nN normal load. Tip-surface resistance scale. <LogR>=9.83.

Roughness measurements are plotted Fig.17 and Fig.18.

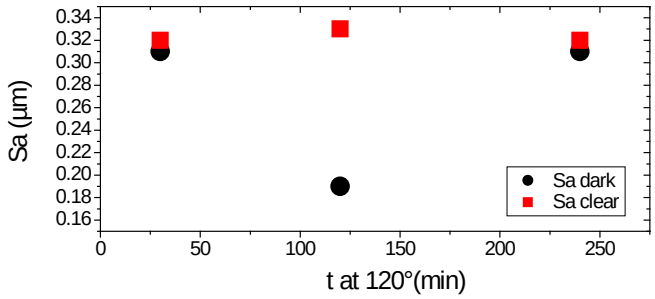

Fig.17: *Sa* roughness parameter for coating [A] deposited with different durations of heat treatment at 120°(NiP/Al substrate). *V*=300mm/min. The surface displays clear zones and dark zones.

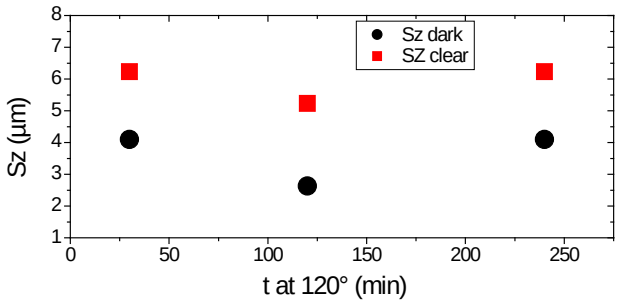

Fig.18: *Sz* roughness parameter for coating [A] deposited with different durations of heat treatment at 120° (NiP/Al substrates. *V*=300mm/min. The surface displays clear zones and dark zones.

The *Sa* value for the different durations of heat treatment is not easy to analyse; they are the same for the dark and clear zones for 30min and 240min and very different for the 120min treatment. More investigations are needed to understand this behaviour. The *Sz* values show higher values for the clear zones as in Fig11.

The 4 point measurements were then performed on the coatings deposited on glass. Fig.19 shows the minimum, maximum and average values of *Rs* measured on a line.

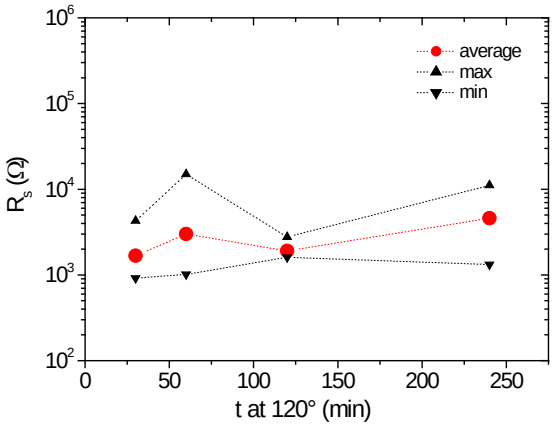

Fig.19: Maximum, minimum and average value of *Rs* for different durations of heat treatment at 120° for coating [A]. *V*=300mm/min.

The lowest average value is measured for the 30min treatment and the highest for the 240min one. The minimum and maximum values on a line vary a lot attesting of the inhomogeneity of the charge distribution. The Rs_{mini} calculated from all the measurements is plotted Fig.20; the minimum value is again 735Ω□ corresponding to a withdrawal speed of 300mm/min and 120min at 120°. A possible explanation would be that the sol is less consolidated with a short treatment at 120° and that the deformation of the layer would allow a closer contact between the charges. This will be taken into account when defining the best parameters.

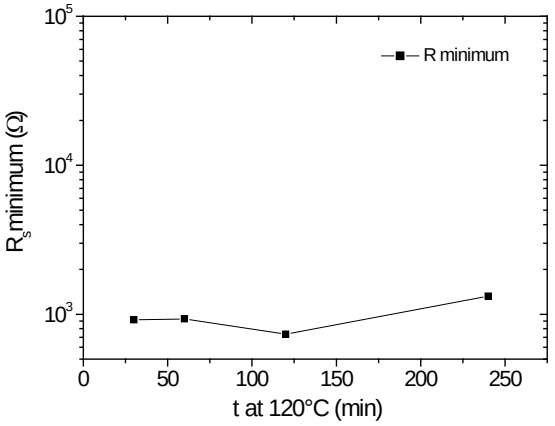

Fig.20: Minimum *Rs* from all measurements when varying the duration of the 120° heat treatment. *V*=300mm/min.

Despite the difficulty in obtaining even layers with sol-gel coating [A] these films were rather conducting. First results of NSS tests showed that they could resist for 1000h before showing the first corrosion pits.

B. Coating [B]

The above results have shown the effect of having two types of fillers in the sol: carbon black with a small form factor and graphite with a much higher one.

It is commonly stated in literature that a filler with a higher form factor lowers the percolation threshold for conduction [10]. Here we observe that a big difference in form factors for a suspension with 2 types of fillers disturbs the dip-coating deposition process. The flow of excess material during withdrawal can carry differently the charges; this prevents a homogeneous film to form.

In order to verify this, a suspension of carbon black [B] has been added to the same precursor in the same conditions for a new sol-gel film deposition.

The coatings were very homogeneous and no dark or clear zone was observed. The roughness parameters *Sa* and *Sz* were measured for coating [B]; we found *Sa*=0.12µm and *Sz*=2.29µm. This is much lower than for coatings [A] (dark or clear zones). The *Sa* value is even lower than for the bare NiP (0.19µm). One can assume that the roughness is filled by the even coating.

The conducting tip AFM images Fig.21 shows a uniform film with high conductivity.

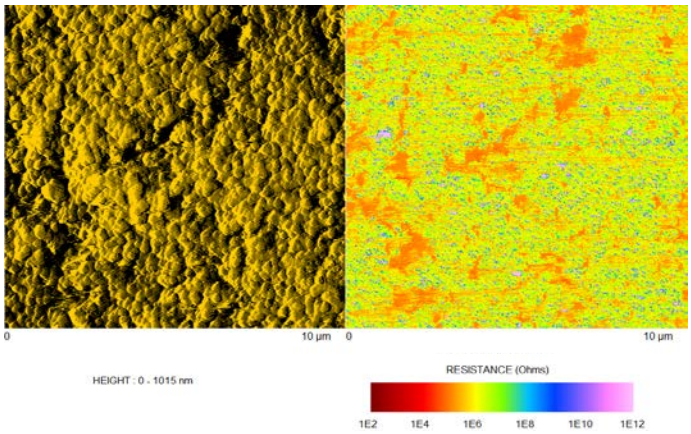

Fig.21: AFM images of sol-gel [B] coating on NiP/Al substrate (300mm/min, 120min-120°). Left) topographic image, right) electrical image, doped diamond tip, 150nN normal load. Tip-surface resistance scale. <LogR>=5.61

The carbon black particles were measured by TEM; they have a diameter of about 50nm and seem to be forming larger nodules.

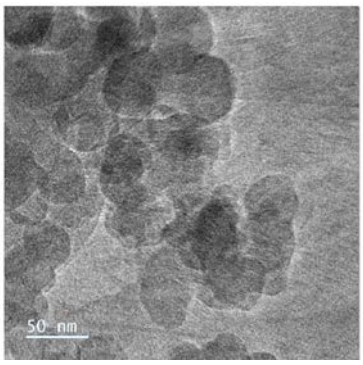

Fig.22: TEM image of suspension [B] deposited on a grid.20kV.

4 point sheet resistance characterizations were performed on coatings deposited on glass slabs. The measurements were done in lines on 4 different samples. They are shown in Fig.23 where *Rs* is plotted versus the position on the coupon. The first measure is at the top of the sample. A very good repeatability is observed. The mean value calculated between point 3 and point 10 is about 1kΩ□.

With coating [A] it was not possible to plot the *Rs* values according to their position on the coupon because of the scattered measurements due to the random presence of large graphite plates. Here with coating [B] the values are rather constant even at the bottom of the coupon. This indicates that no major bulge has accumulated at the bottom of the sample.

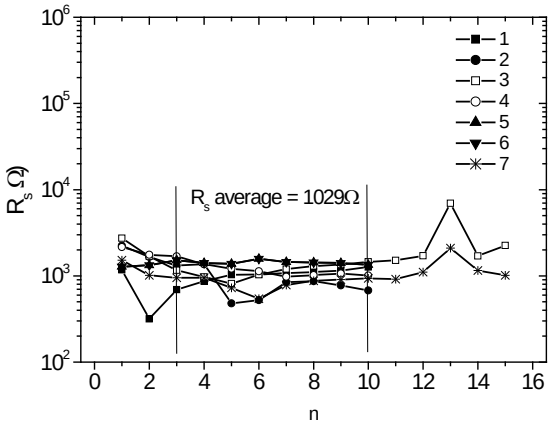

Fig.23: Series at different locations of *Rs* measurements on coating [B] starting from the top of the sample towards the bottom. *V*=300mm/min, 60min at 60° and 120min at 120°.

NSS tests for this coating are still running and not yet analysed.

IV. CONCLUSION

First work had shown it was possible to deposit a hybrid sol-gel coating on NiP/Al coupons by selecting proper precursors such as GPTMS and TPOZ. By tuning the process parameters, the viscosity of the sol, the dip-coating conditions and the consolidation treatment it was possible to obtain a multi-functional coating. A proof of concept has been made with deposits impervious to 1000h of neutral salt spray and allowing electrical continuity. The aim of this large ongoing study is to obtain conducting and anti-corrosion coatings to replace the cadmium/chromium VI finish of certain connector housings. The formulation of the initial study had to be modified because of the issue of carbon black powder in an industrial context. The powder was replaced by water suspensions which changes many of the fine tunings of the formulation. Moreover, the anti-corrosion and conduction properties are often contradictory which requires multiple adjustments to keep both properties as required by specifications. We have shown here that deposition of an even sol-gel coating by the dip-coating was much easier with a single type of small form factor particles. Further work has to concentrate on the anti-corrosion and the mechanical/tribological properties of such coatings.

ACKNOWLEDGEMENTS

The authors wish to thank the DGA-RAPID program (régime d'appui pour l'innovation durable) for funding the CadSTAR project.

REFERENCES

[1] https://echa.europa.eu/information-on-chemicals/euclef
[2]https://echa.europa.eu/fr/substances-restricted-under-reach/-/dislist/details/0b0236e1807e2518
[3] D. Bryce Mitton, A. Carangelo, A. Acquesta, T. Monetta, M. Curioni, F. Bellucci, "Selected Cr(VI) replacement options for aluminium alloys: a literature survey", Corros. Rev. 35, 6, 2017, pp. 365-381.
[4] R. B. Figueira, C.R.J. Silva, E.V. Perreira, "Organic-inorganic hybrid sol-gel coatings for metal corrosion protection: a review of recent progress", J. Coatings Technol. Res, 12, 2015, pp. 1-35.
[5] C.J. Brinker and G.W. Scherer, "Sol-Gel Science, The Physics and Chemistry of Sol-Gel Processing", 1990. Gulf Professional Publishing.
[6] C. Genet, "Revêtements multifonctionnels par voie sol-gel pour connecteurs électriques en AA6061-T6s", thèse Université Toulouse 3- Paul Sabatier, 2019.
[7] C. Genet, M. J. Menu, O. Gavard, F. Ansart, M Grésier, R. Montpellaz, "Innovative formulation combining Al, Zr, and Si precursors to obtain anticorrosion hybrid sol-gel coatings", Molecules, 23, 1135, 2018, pp. 1-15.
[8] C. Genet, H. Azougaghe, M. Gressier, F. Ansart, O. Gavard, M. J. Menu, " State of the art and recent advances in electrical conductive coatings by sol-gel Process", Journal of Material Sciences and Engineering, Vol. 10.5; 2021, pp. 1-12.
[9] L. Landau, B. Levich, "Dragging of a liquid by a moving plate", Dyn. Curved Front, 1988, pp. 141-153.
[10] E. Enriquez, J. de Frutos, J.F. Fernandez, M.A. De La Rubia, "Conductive coatings with low carbon-black content by adding carbon nanofibers", Compos. Sci. Technol. 93, 2014, pp. 9-16.